The EMBO Journal Vol.18 No.19 pp.5252–5263, 1999

Cathepsin D targeted by acid sphingomyelinase-derived ceramide

Michael Heinrich, Marc Wickel, Wulf Schneider-Brachert[1], Christiane Sandberg, Julie Gahr, Ralf Schwandner[2], Thomas Weber[3,4], Josef Brunner[3], Martin Krönke[5] and Stefan Schütze[6]

Institute of Immunology, University of Kiel, Kiel, Germany and [3]Department of Biochemistry, Swiss Federal Institute of Technology, Zürich (ETHZ), Switzerland

[1]Present address: Institute of Medical Microbiology and Hygiene, University of Regensburg, Germany
[2]Present address: Tularik Inc., South San Francisco, CA 94080, USA
[4]Present address: Memorial Sloan-Kettering Cancer Center, New York, NY 10021, USA
[5]Present address: Institute of Medical Microbiology and Hygiene, University of Cologne, Germany

[6]Corresponding author
e-mail: schuetze@immunologie.uni-kiel.de

M.Heinrich and M.Wickel contributed equally to this work

Ceramide has been recognized as a common intracellular second messenger for various cytokines, growth factors and other stimuli, such as CD95, chemotherapeutic drugs and stress factors. To understand the role of ceramide during apoptosis and other cellular responses, it is critically important to characterize direct targets of ceramide action. In this paper, we show that ceramide specifically binds to and activates the endosomal acidic aspartate protease cathepsin D. Direct interaction of ceramide with cathepsin D results in autocatalytic proteolysis of the 52 kDa pre-pro cathepsin D to form the enzymatically active 48/32 kDa isoforms of cathepsin D. Acid sphingomyelinase (A-SMase)-deficient cells show decreased cathepsin D activity, which could be reconstituted by transfection with A-SMase cDNA. The results of our study identify cathepsin D as the first endosomal ceramide target that colocalizes with and may mediate downstream signaling effects of A-SMase.

Keywords: acid sphingomyelinase/cathepsin D/ceramide/TID-ceramide

Introduction

Ceramide has emerged as an intracellular signal mediator transducing the effects of various exogenous stimuli including cytokines such as tumor necrosis factor (TNF), interferon (IFN)-γ, interleukin (IL)-1, nerve growth factor, or CD28 and CD95 (Fas/APO-1) receptor triggering, ionizing radiation, glucocorticoids, anti-cancer drugs and serum deprivation (Liu *et al*., 1997; Perry and Hannun, 1998). The biological responses to ceramide range from induction of proliferation and differentiation to cell-cycle arrest. The most prominent yet controversial role of ceramide is the induction of apoptosis in various cell types (Obeid *et al*., 1995; reviewed in Hannun and Obeid, 1995; Kolesnick and Krönke, 1998). The production of ceramide is mediated either by *de novo* synthesis, involving ceramide synthase located in the endoplasmic reticulum (ER) and mitochondria, or by hydrolysis of sphingomyelin-engaging sphingomyelinase (SMase; Spiegel and Merrill, 1996). Ligand binding to the p55 TNF receptor (TR55), interleukin-1 receptor 1 (IL-1 RI) and the Fas receptor results in the activation of two SMases, a plasma-membrane-bound neutral SMase (N-SMase) and an endolysosomal acid SMase (A-SMase; Schütze *et al*., 1992; Wiegmann *et al*., 1994; Cifone *et al*., 1995; Liu and Anderson, 1995). Each type of SMase generates the second messenger ceramide with, however, different kinetics and, most importantly, at different intracellular locations. Structure–function analysis of the cytoplasmic domain of TR55 revealed that specific TNF-receptor domains link to the respective SMases and to diverse signaling pathways (Wiegmann *et al*., 1994). N-SMase activation is coupled to a neutral sphingomyelinase activation domain (NSD), via the adaptor protein FAN (Adam-Klages *et al*., 1996; Kreder *et al*., 1999). The domain of TR55 activating A-SMase corresponds to the death domain that binds the adaptor protein TRADD, which in turn recruits a further protein, FADD, to activate caspase 8 and A-SMase (Schwandner *et al*., 1998). Fibroblasts derived from FADD-deficient mice are defective in TNF-induced A-SMase activation (Wiegmann *et al*., 1999). Notably, the apoptotic caspase 8 seems not to be involved in the A-SMase activation pathway (Schwandner *et al*., 1998). The signaling cascade downstream of ceramide may, however, involve caspase 3 (CPP32; Smyth *et al*., 1996). A role for A-SMase in transmitting apoptotic signals in response to Fas/CD95, γ-irradiation, TNF and lipopolysaccharide (LPS) has been suggested by several reports (Cifone *et al*., 1995; Santana *et al*., 1996; Haimovitz-Friedmann *et al*., 1997; Herr *et al*., 1997; De Maria *et al*., 1998; Monney *et al*., 1998). However, direct evidence linking ceramide signaling to specific effector elements of the apoptotic response remains to be provided. As to possible signaling functions of endosomal A-SMase the question arises as to whether ceramide signals across the endosomal membrane or targets proteins in the endosomal lumen.

Understanding the role of ceramide during apoptosis and other cellular responses crucially requires identification of the direct targets of ceramide. In this regard, proteins physically interacting with ceramide produced by A-SMase remained particularly elusive. Several enzymes have been described recently that can be activated by ceramide including a ceramide-activated protein kinase (CAPK; Mathias *et al*., 1991) that has been suggested to

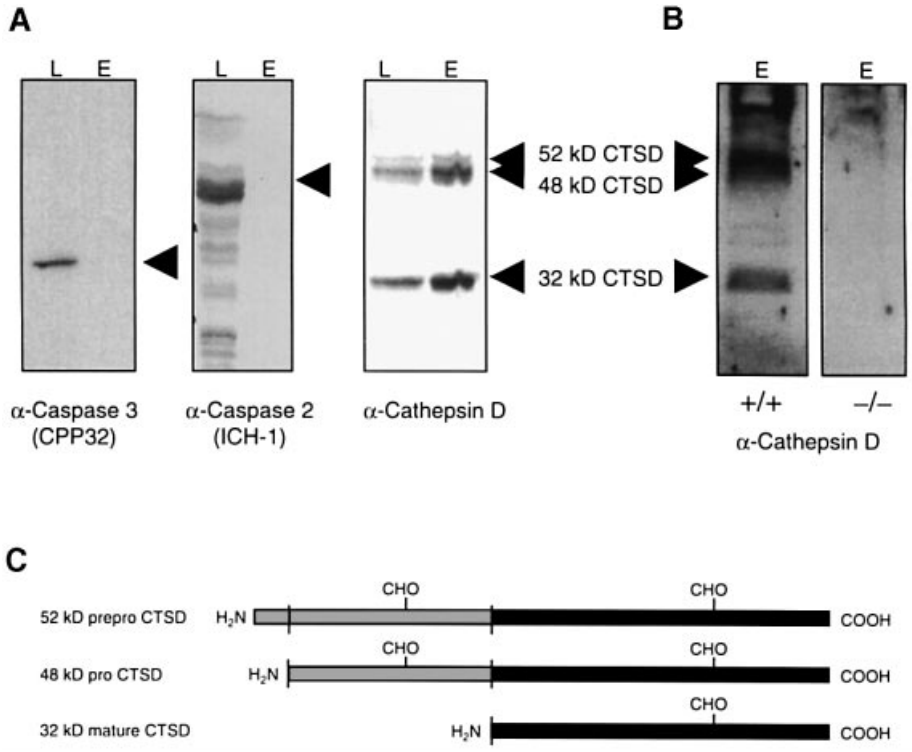

Fig. 1. Human CTSD selectively binds to ceramide–Sepharose. Immunoblot analysis of lysates (L) and ceramide-affinity eluates (E) from (**A**) U937 cells and (**B**) kidneys derived from wild-type C57 BL/6 (+/+) or CTSD-deficient C57BL/6J mice (–/–). U937 cells and kidneys were homogenized, nuclei-free lysates prepared and proteins were subjected to ceramide-affinity chromatography followed by elution with an excess of D-*erythro*-ceramide and analyzed by 10% SDS–PAGE. Equal amounts of protein from each fraction were loaded. Western blotting was performed using mAbs against human caspase 2, caspase 3 and polyclonal antibodies specific for human CTSD (U937 cells) or polyclonal anti-murine CTSD antibodies (murine cellular lysates). The data shown are representative of four independent experiments. (**C**) Characteristic features of different processing forms of CTSD.

be related or identical to the kinase suppressor of Ras (KSR; Zhang *et al*., 1997). Further ceramide-responsive proteins include protein phosphatase 2A (CAPP; Dobrowski *et al*., 1993; Law *et al*., 1995), protein kinase Cζ (Müller *et al*., 1995), protein kinase Raf-1 (Huwiler *et al*., 1996; Müller *et al*., 1998), the stress-activated/c-*jun* N-terminal protein kinase (JNK; Westwick *et al*., 1995; Huang *et al*., 1997; Schütze *et al*., 1999) and a CPP32 (caspase 3)-like apoptotic protease (Mizushima *et al*., 1996; Smyth *et al*., 1996; Zhang *et al*., 1996; Anjum *et al*., 1998). Evidence for a direct physical interaction of ceramide has been difficult to obtain (Müller *et al*., 1995, 1998; Huwiler *et al*., 1996). In particular, in most studies the specificity of ceramide binding and activation of the target proteins have not been demonstrated with competitive lipids or ceramide isomers.

In the present study we sought specific ceramide targets that colocalize with the subcellular site of A-SMase. Ceramide-affinity chromatography revealed cathepsin D (CTSD) as a novel ceramide-binding protein. Using D-*erythro*-ceramide-based photo-crosslinking, we provide evidence for the specific interaction of ceramide with CTSD, leading to enhanced enzymatic activity. CTSD is endosomally active and involved in the proteolytic activation of proteins to be secreted. CTSD has recently been implicated in mediating apoptosis in response to TNF, IFN-γ, CD95 (Deiss *et al*., 1996), chemotherapeutic agents, such as etoposide and adriamycin (Wu *et al*., 1998), and serum deprivation (Shibata *et al*., 1998; Ohsawa *et al*., 1999). In conclusion, CTSD may link A-SMase to the secretory pathway and to apoptotic signaling events.

Results

Ceramide selectively interacts with CTSD

One controversy over ceramide action concerns its role in apoptotic cell death. Recently, apoptotic proteases of the caspase family (CPP32/caspase 3) have been suggested to serve as targets downstream of ceramide (Mizushima *et al*., 1996; Smyth *et al*., 1996; Zhang *et al*., 1996; Anjum *et al*., 1998). To investigate the ceramide-binding profile of specific apoptotic proteases, we developed a ceramide-affinity chromatography by covalently coupling D-*erythro*-sphingosine via an aminohexanoic acid spacer to activated Sepharose 4B, resulting in an immobilized short chain (C6-) D-*erythro*-ceramide. Proteins eluted from the affinity matrix were analyzed using SDS–PAGE and immunoblotting. As shown in Figure 1A, neither ICH-1 (caspase 2) nor CPP32 (caspase 3) could be enriched by ceramide-affinity chromatography of lysates from U937 cells. In contrast, the aspartic protease CTSD, which was recently shown to be associated with the apoptotic pathway (Deiss *et al*., 1996; Wu *et al*., 1998), bound to and was specifically eluted from the ceramide-affinity matrix by competition with an excess of D-*erythro*-ceramide (Figure 1A). CTSD did not elute from the matrix when the biologically inactive D-*erythro*-dihydroceramide (Bielawska *et al*., 1993) or D-*erythro*-dihydrosphingosine were used as competitors.

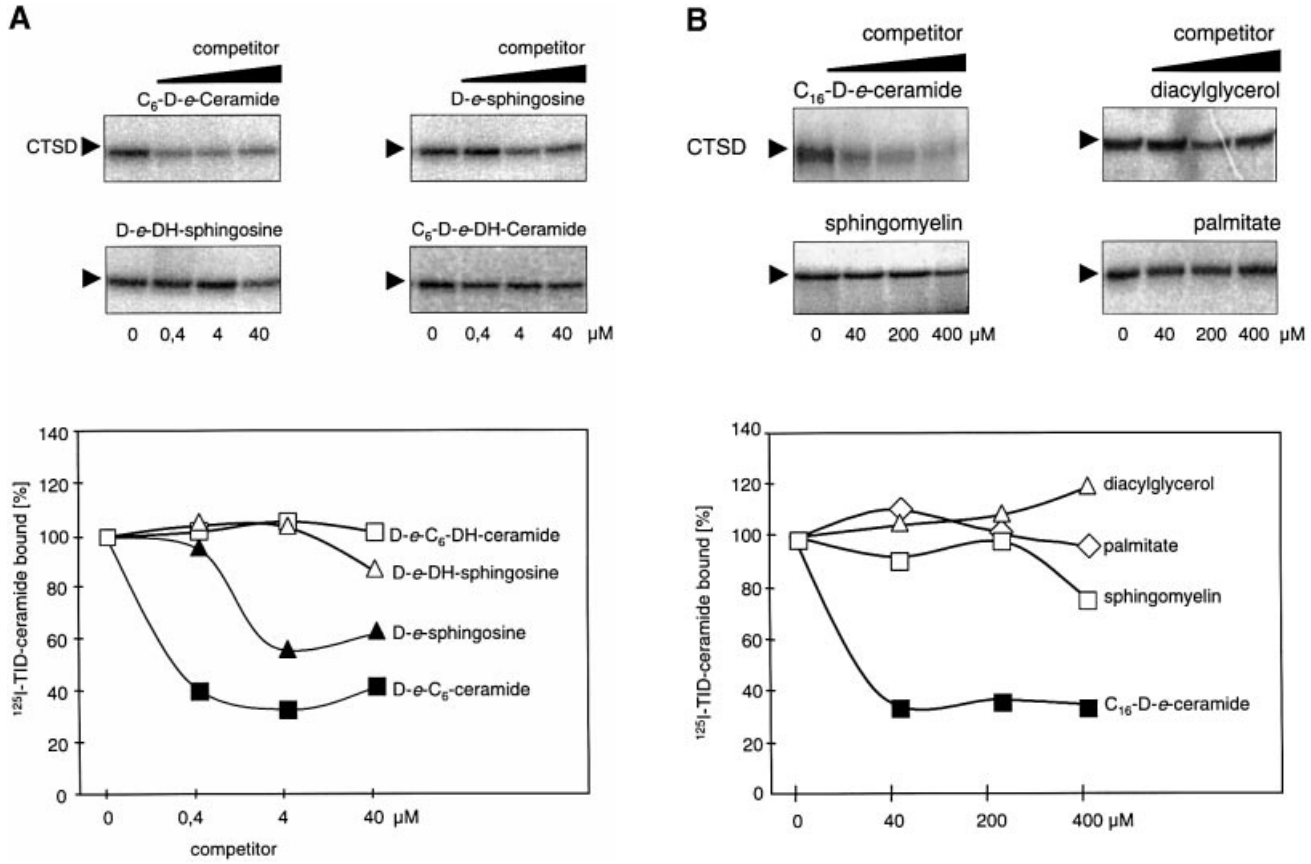

Fig. 2. Binding of radiolabeled TID-ceramide to CTSD. To determine the specificity of [^{125}I]TID-ceramide association to purified human CTSD *in vitro*, competition assays with unlabeled lipids were performed by incubation of 2 µg CTSD from human liver with 1 µCi (0.5 pmol) [^{125}I]TID-ceramide in a volume of 25 µl alone or in the presence of 0.4–40 µM of unlabeled lipids: D-*erythro*-C_6-ceramide (■), D-*erythro*-sphingosine (▲), D-*erythro*-C_6-dihydroceramide (□) and D-*erythro*-dihydrosphingosine (△) (**A**), and 40–400 µM of D-*erythro*-C_{16}-ceramide (■), 1,2-diacylglycerol (△), sphingomyelin (□) or palmitate (◇) (**B**). Samples were UV-crosslinked and binding of radiolabeled TID-ceramide analyzed by SDS–PAGE and autoradiography. Autoradiographs of the 32 kDa CTSD–TID-ceramide complex are shown in the upper panels, in the lower panel the amount of [^{125}I]TID-ceramide binding was calculated as a percentage binding in the absence of unlabeled competitor.

In addition, CTSD did not bind to an affinity matrix composed of D-*erythro*-dihydroceramide (data not shown).

CTSD is the major aspartic protease of endolysosomes. The protease is synthesized and translocated into the ER as an inactive pre-proenzyme (52 kDa) that is subsequently converted into an active, intermediate proenzyme (48 kDa) in endosomal compartments (Gieselmann *et al*., 1983; Rijnboutt *et al*., 1992). Further cleavage in late endosomes and lysosomes generates the mature form of 32 kDa (Figure 1C). Notably, all three isoforms of CTSD appeared in the ceramide eluates, suggesting that the ceramide-binding site localizes within the 32 kDa CTSD polypeptide. After incubation with ceramide–Sepharose, the lysates were almost completely depleted of CTSD, indicating effective binding of cellular CTSD to the ceramide matrix (not shown). None of the CTSD isoforms could be eluted from the ceramide–Sepharose matrix when loaded with lysates from kidney cells of CTSD-deficient mice (Figure 1B). This provides further evidence for the identity of the eluted ceramide-binding proteins with CTSD.

Specificity of ceramide binding to CTSD

Direct and specific binding of ceramide to CTSD was additionally assessed using the radiolabeled photo-crosslinking ceramide analog, 3-trifluoromethyl-3-(*m*-iodophenyl) diazirine D-*erythro*-sphingosine ([^{125}I]TID-ceramide) as the ligand (Weber and Brunner, 1995). This radiolabeled ceramide analog has previously been used to show the association of ceramide with the cytosolic protein kinase Raf-1 (Huwiler *et al*., 1996). To demonstrate specific ceramide binding to CTSD, purified human 32 kDa CTSD was photoaffinity labeled with [^{125}I]TID-ceramide and analyzed on SDS–PAGE (Figure 2). Labeling of CTSD with [^{125}I]TID-ceramide allowed us to perform specificity analysis of ceramide binding to CTSD using different ceramide and sphingosine isomers and various unrelated lipids. Photo-crosslinking with [^{125}I]TID-ceramide was performed in the presence of increasing amounts of synthetic D-*erythro*-C_6-ceramide, D-*erythro*-C_6-dihydroceramide, D-*erythro*-sphingosine, D-*erythro*-dihydrosphingosine, palmitic acid, 1,2-diacylglycerol and sphingomyelin. As shown in Figure 2A, D-*erythro*-C_6-ceramide and D-*erythro*-sphingosine dose-dependently competed for binding of the radiolabeled [^{125}I]TID-ceramide, whereas the biologically inactive D-*erythro*-dihydroceramide and D-*erythro*-dihydrosphingosine were significantly less potent in competing for TID-ceramide binding to CTSD. These results suggest that the 4,5-*trans* double bond within the sphingoid backbone of D-*erythro*-ceramide is important for the binding of ceramide to CTSD. At lower doses of competitor, D-*erythro*-C_6-ceramide was more effective in competing for [^{125}I]TID-ceramide binding than D-*erythro*-

sphingosine (Figure 2A), suggesting a prevalent role of ceramide over sphingosine as the ligand for CTSD. Long-chain D-*erythro*-C_{16}-ceramide (Figure 2B) competed for ceramide binding as efficiently as D-*erythro*-C_6-ceramide, suggesting that the length of the fatty acid chains of the D-*erythro*-ceramides has no major effect on the competing capacity. The free fatty acid palmitate did not compete for [^{125}I]TID-ceramide binding to CTSD, which is consistent with the previous notion that the alkyl chain of the sphingoid backbone, rather than the acyl chain, interacts with ceramide-binding proteins (Krönke, 1997). Other lipids, such as 1,2-diacylglycerol and sphingomyelin, also did not displace [^{125}I]TID-ceramide from CTSD binding.

[^{125}I]TID-ceramide did not react with recombinant CPP32 (caspase 3; not shown), consistent with the inability of caspase 3 to bind to the ceramide-affinity chromatograph (Figure 1).

Ceramide stimulates CTSD activity

To investigate the functional consequences of ceramide binding to CTSD, methods were developed that allowed measurement of the specific enzymatic activity of CTSD in whole cells, in cellular lysates or of the purified enzyme.

To detect CTSD activity in whole cells, proteolysis of the cell-permeable peptide glycine–leucine–rhodamine 110 (CellProbe GL*cathepsin D enzyme substrate, Coulter), resulting in formation of fluorescence, was analyzed by flow cytometry. The effect of exogenous ceramide on cellular CTSD activity was estimated by incubating U937 cells for 4 h with 100 μM D-*erythro*-C_6-ceramide and 100 μM D-*erythro*-C_6-dihydroceramide. As shown in Figure 3A, D-*erythro*-C_6-ceramide, but not D-*erythro*-C_6-dihydroceramide, stimulated CTSD proteolytic activity, which is in line with the requirement of the 4,5-*trans* double bond for biological activity of D-*erythro*-ceramide.

The CTSD activation in intact cells by D-*erythro*-C_6-ceramide and D-*erythro*-sphingosine was dose-dependent with half-maximal effects at a concentration of 30 μM. Again, D-*erythro*-dihydroceramide and D-*erythro*-dihydrosphingosine were inactive (Figure 3B).

No CTSD activity was detected in fibroblasts derived from CTSD-deficient mice (CTSD$^{-/-}$; Figure 3C). CTSD activity was reconstituted in CTSD$^{-/-}$ fibroblasts transfected with CTSD cDNA (CTSD$^{-/-}$ pCTSD), revealing the specificity of this assay for CTSD.

To measure CTSD-specific protease activity *in vitro*, an independent assay was established using purified human parathyroid hormone 1–84 (PTH) as substrate. Digestion of PTH with CTSD results in cleavage of the hormone between Phe34 and Val35 yielding PTH (1–34) and PTH (35–84) fragments (Figure 4A; Zull and Chuang, 1985; Hamilton *et al*., 1986). Proteolysis of the intact hormone was detected by immunoblotting using a monoclonal antibody (mAb) generated against peptide 1–34. As shown in Figure 4B, incubation of human PTH with lysates from HeLa cells overexpressing CTSD resulted in proteolysis of PTH starting after 30 min. PTH proteolysis could be blocked by the aspartate-protease inhibitor pepstatin A, a selective inhibitor of CTSD (Conner, 1989; Metcalf and Fusek, 1993; M.Heinrich, M.Wickel and S.Schütze, unpublished observations).

The potency and selectivity of D-*erythro*-C_6-ceramide

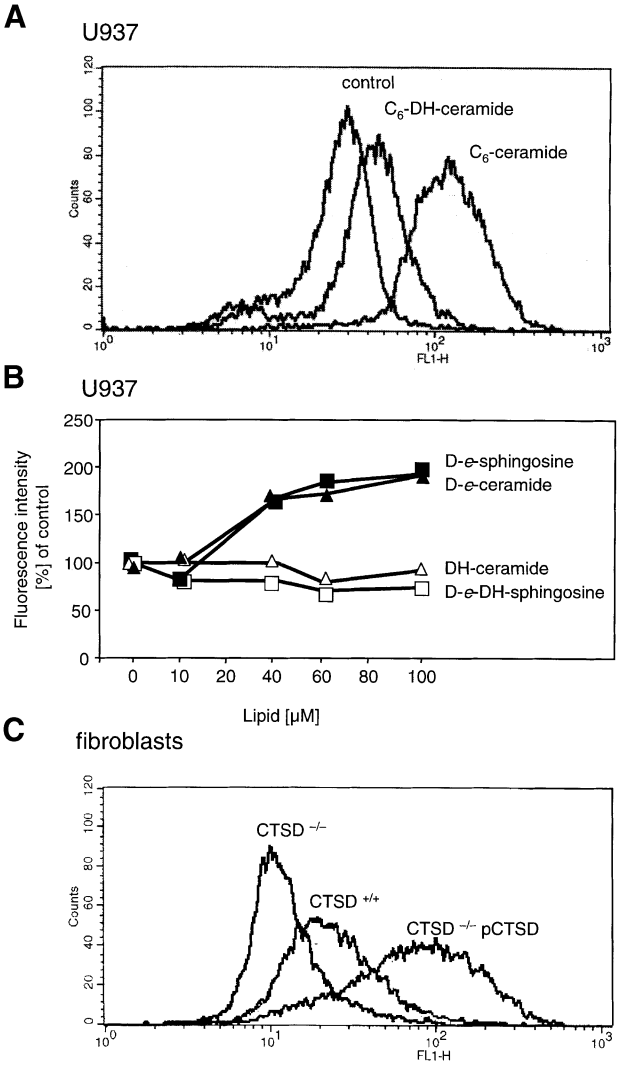

Fig. 3. Ceramide stimulates CTSD enzymatic activity in intact cells. (**A**) To estimate the effect of ceramide on enzymatic activity of CTSD in whole cells, U937 cells were left untreated or were incubated with 100 μM D-*erythro*-C_6-ceramide and D-*erythro*-C_6-dihydroceramide in DMSO for 4 h. Cells were then stained with CellProbe GL*cathepsin D enzyme substrate (Coulter) and proteolysis of the peptide glycine–leucine–Rho 110 was estimated by flow cytometry (Becton-Dickinson FACSCalibur). (**B**) The dose-effect of increasing concentrations of D-*erythro*-C_6-ceramide (▲), D-*erythro*-sphingosine (■), D-*erythro*-C_6-dihydroceramide (△) and D-*erythro*-dihydrosphingosine (□) in DMSO was determined as in (A) and the shift in fluorescence calculated as a percentage of the DMSO-treated controls. (**C**) To determine the CTSD specificity of the assay, fibroblasts from CTSD-deficient mice (CTSD$^{-/-}$), wild-type mice (CTSD$^{+/+}$) or CTSD$^{-/-}$ fibroblasts retransfected with the CTSD cDNA (CTSD$^{-/-}$ pCTSD) were assayed by flow cytometry.

to stimulate CTSD enzymatic activity directly were also revealed when ceramide, incorporated into PC liposomes, was added either to lysates from HeLa cells overexpressing CTSD or to purified CTSD (Figure 4C and D). In both cases, D-*erythro*-ceramide, but not D-*erythro*-dihydroceramide, enhanced CTSD proteolytic activity. Pepstatin A blocked ceramide-induced PTH digestion confirming the specificity of action of ceramide towards CTSD. Together, our findings suggest that ceramide directly stimulates CTSD enzymatic activity in intact cells, in cellular lysates and purified CTSD protein.

To dissect the specificity of ceramide and sphingosine

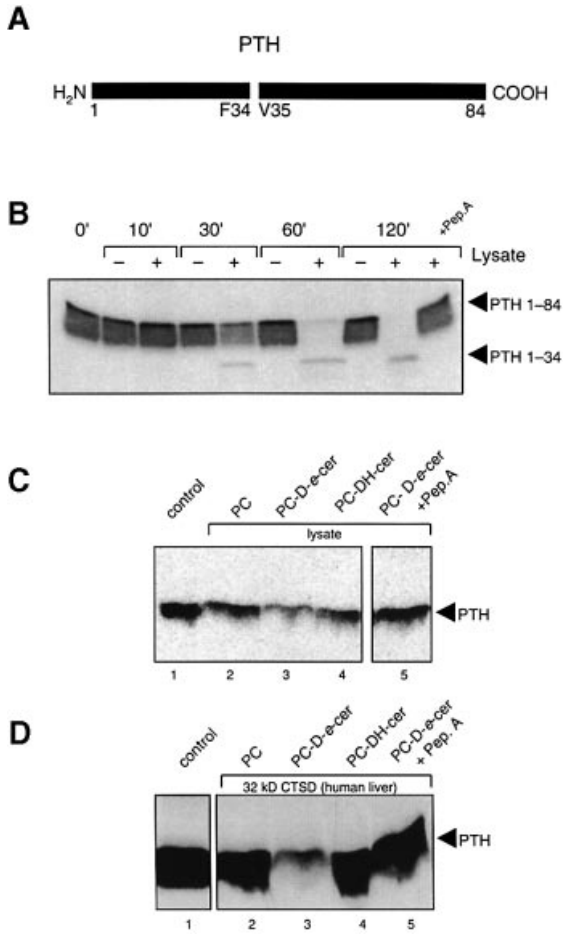

Fig. 4. Ceramide activates CTSD *in vitro*. (**A**) Structure of PTH consisting of a 34 aa fragment (1–34) and a 50 aa fragment (35–84). (**B**) Kinetics of PTH digestion. Lysates from HeLa cells overexpressing CTSD were incubated in acidic buffer for the times indicated in the presence of 50 ng PTH as substrate. Aliquots were separated by SDS–PAGE and the amount of PTH was assayed by immunoblotting using anti-PTH mAb (peptide 1–34) and the ECL detection system (Amersham). (**C**) The effect of ceramide on endogenous cellular CTSD was assayed by incubating human PTH as substrate alone or with lysates from HeLa cells overexpressing CTSD at pH 4.2 for 30 min at 37°C to allow for autoproteolysis of pre-pro CTSD. D-*erythro*-C_6-ceramide or D-*erythro*-C_6-dihydroceramide complexed to PC liposomes (1 mM ceramide/9 mM phosphatidylcholine) was added and incubation was continued for a further 6 min. (**D**) The effect of ceramide on purified CTSD *in vitro* was assayed by incubating purified human liver CTSD for 6 min together with PTH as substrate in the absence or presence of D-*erythro*-C_6-ceramide or D-*erythro*-C_6-dihydroceramide each complexed to PC liposomes (1:9). To demonstrate CTSD specificity of the reactions, 0.5 μM pepstatin A was added to the assay as indicated.

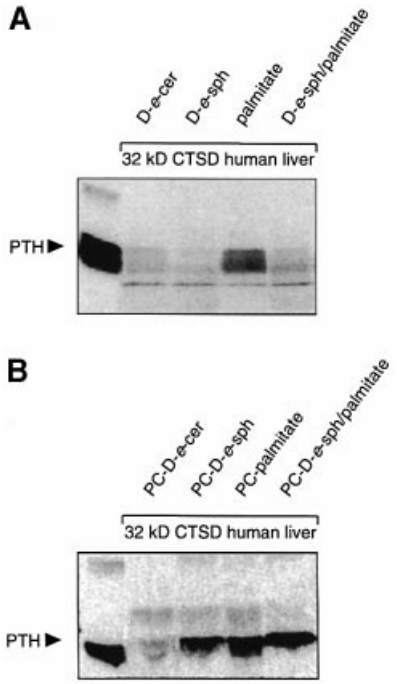

Fig. 5. CTSD responds to sphingosine in solution but not to sphingosine in PC liposomes. The effects of ceramide, sphingosine and palmitate on purified CTSD *in vitro* were assayed by incubating purified human liver CTSD for 6 min together with 50 ng PTH as substrate in the absence or presence of 60 μM each of D-*erythro*-C_6-ceramide, D-*erythro*-sphingosine or palmitate in DMSO (**A**), or each lipid complexed in phosphatidylcholine liposomes (at 1 mM/9 mM PC) (**B**). Aliquots were separated by SDS–PAGE and the amount of PTH was assayed by immunoblotting using anti-PTH mAb (peptide 1–34) and the ECL detection system (Amersham) as in Figure 4.

effects we investigated the potency of D-*erythro*-ceramide and D-*erythro*-sphingosine to stimulate CTSD activity under different conditions. As shown in Figure 5, both ceramide and sphingosine are capable of stimulating CTSD enzymatic activity when applied in dimethylsulfoxide (DMSO) (Figure 5A); however, only ceramide, not sphingosine, stimulates CTSD when incorporated into detergent-free lipid bilayers. The free fatty acid palmitate is inactive in DMSO as well as in PC-liposomes either alone or in combination with sphingosine (Figure 5B). These observations indicate that in a lipid environment, the fatty acid chain of ceramide is required for association with the liposomal bilayer, possibly to ensure a proper orientation of the molecule required for CTSD interaction with the alkyl chain of ceramide.

The PTH assay appears to be specific for CTSD in crude cellular lysates because in homogenates from CTSD-deficient fibroblasts, PTH was not degraded (Figure 6A). In contrast, in $CTSD^{-/-}$ fibroblasts reconstituted with CTSD cDNA, PTH was degraded completely (Figure 6B). The levels of CTSD expression in both cell lines were monitored by immunoblotting, demonstrating that the $CTSD^{-/-}$ fibroblasts used in these assays were completely depleted of the enzyme (Figure 6A and B).

Ceramide-induced post-transcriptional maturation of CTSD

The processing of CTSD from the 52 kDa precursor to the mature 32 kDa isoform is one hallmark of CTSD activation. As shown in Figure 7A, incubation of U937 cells with ceramide induced an increase of the mature 32 kDa isoform of CTSD within 4 h. After 8 h, the ceramide-mediated increase in 32 kDa CTSD was ~2.4-fold (Figure 7B). A slight increase in 52 kDa pre-pro CTSD was also observed, which possibly reflects enhanced resynthesis of the precursor as a consequence of increased ceramide-induced production of the 32 kDa mature isoform. These data suggest that ceramide induces CTSD enzymatic activity by triggering proteolytic processing of the CTSD to yield mature and active CTSD. Similar results were obtained using *in vitro* transcribed and translated pre-pro CTSD. Incubation of the radiolabeled protein in an acidic micellar *in vitro* system in the presence of C_6-

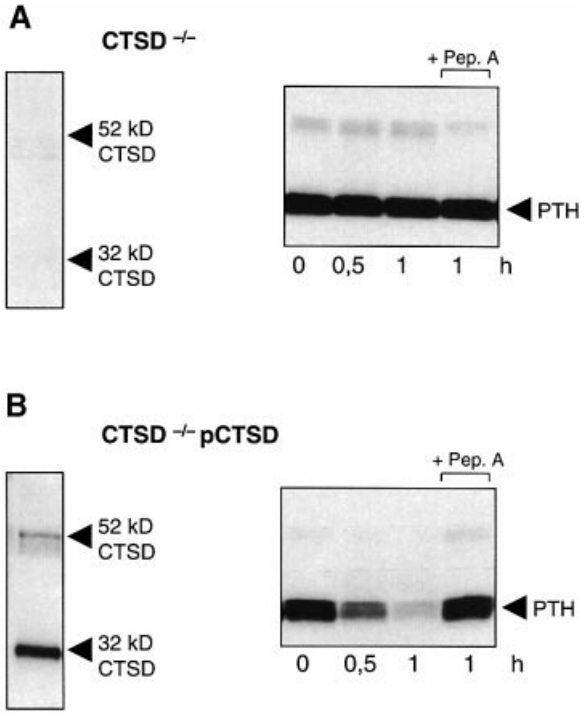

Fig. 6. PTH is a specific substrate for CTSD. To determine the CTSD specificity of PTH proteolysis, lysates from CTSD$^{-/-}$ fibroblasts (**A**) or CTSD$^{-/-}$ fibroblasts reconstituted with CTSD cDNA (**B**) were incubated at pH 4.2 with 50 ng PTH as substrate for the times indicated in the absence and presence of 0.5 μM pepstatin A. Expression of CTSD protein was estimated by immunoblotting using polyclonal anti-CTSD antibody. The level of PTH protein was estimated by immunoblotting using anti-PTH mAb (peptide 1–34).

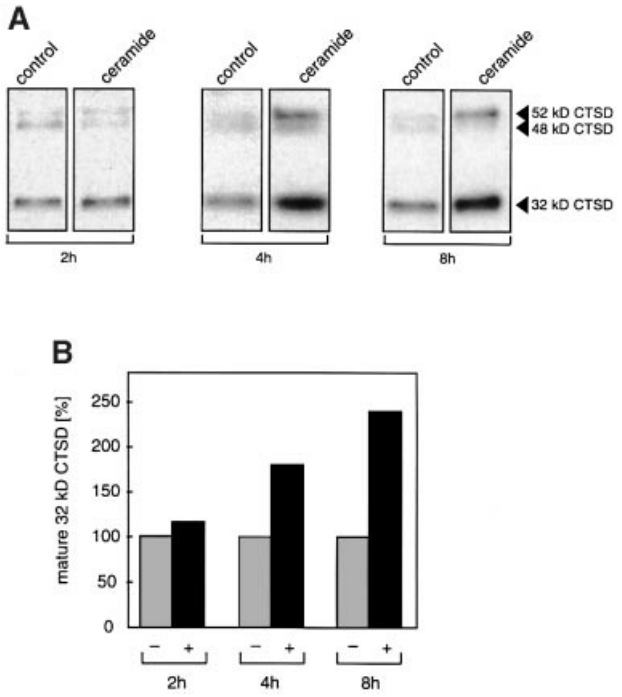

Fig. 7. Ceramide induces maturation of CTSD. (**A**) U937 cells were left untreated or were incubated with 100 μM D-*erythro*-C_6-ceramide in DMSO for 2, 4 and 8 h. Total cell lysates were subjected to SDS–PAGE and analyzed for CTSD isoform expression by immunoblotting. (**B**) CTSD levels were analyzed by two-dimensional laser scanning (Molecular Dynamics Personal Densitometer). The increase in mature 32 kDa CTSD was estimated using the PC-BAS TINA program (Raytest) and calculated as a percentage increase over untreated controls.

ceramide resulted in an enhancement of pre-pro CTSD autoproteolysis, which was already evident after 30 min of incubation (Figure 8A). Finally, lysates from HeLa cells overexpressing pre-pro CTSD showed autoproteolysis of native 52 kDa pre-pro CTSD to form the 48 kDa propeptide and further maturation to 32 kDa CTSD within 10 min *in vitro* (Figure 8B). The 52/48 kDa CTSD conversion was specifically inhibited by the aspartate protease inhibitor pepstatin A, but not by antipain or serine-, cysteine- or metalloprotease inhibitors (Boehringer Complete Protease Inhibitor Cocktail; data not shown). These observations indicate that the processing of pre-pro CTSD occurs autoproteolytically, not requiring other proteases. Ceramide treatment of the lysates again resulted in enhanced production of the 32 kDa mature isoform (Figure 8B).

Together, our data suggest that ceramide is able to induce autocatalytic processing of pre-pro CTSD.

CTSD activity is functionally coupled to A-SMase

Because of its endolysosomal location, CTSD was sensed as a possible target of A-SMase-derived ceramide. In order to evaluate whether A-SMase regulates CTSD activity and processing, we analyzed CTSD activity in an Epstein–Barr virus (EBV)-transformed B-cell line. When compared with the control B-lymphoblast cell line JY, A-SMase-deficient cells from a Niemann–Pick patient expressed similar levels of 52 kDa pre-pro CTSD and 32 kDa mature form, yet lacked almost completely the 48 kDa intermediate pro CTSD isoform (Figure 9B). When assayed for enzymatic CTSD activity using PTH as substrate, markedly reduced PTH cleavage was observed in Niemann–Pick lymphoblasts compared with JY cells (Figure 9C, lanes 3 and 2, respectively). When A-SMase activity was restored in A-SMase-deficient Niemann–Pick clone MS1418 by transfection with A-SMase cDNA, high levels of 48 kDa CTSD protein were again observed (Figure 9B), corresponding to elevated enzymatic activity of CTSD (Figure 9C, lane 4). The 48 kDa form represents the enzymatically active membrane-bound CTSD isoform. Together, our data suggest a functional association of A-SMase activity and pre-pro CTSD processing in lymphoblasts.

In contrast to Niemann–Pick cells that are defective in ceramide production based on defective A-SMase activity, fibroblasts from patients affected with Farber lipogranulomatosis contain high levels of ceramide based on the reduced acid ceramidase activity (van Echten-Deckert *et al*., 1997). Enhanced CTSD activity was observed in Farber fibroblasts (F92/5) compared with control fibroblasts (F19/17; Figure 9D). This finding provides further evidence for a role of intracellular ceramide in the regulation of CTSD activity.

The functional link between A-SMase and CTSD processing also became apparent when A-SMase activity was blocked by the tricyclic antidepressant desipramine, an agent that induces proteolytic degradation and irreversible down-modulation of A-SMase (Hurwitz *et al*., 1994). As shown in Figure 10, desipramine pretreatment of HeLa cells resulted in a dose-dependent reduction of the levels of mature 32 kDa CTSD with concomitant increments in

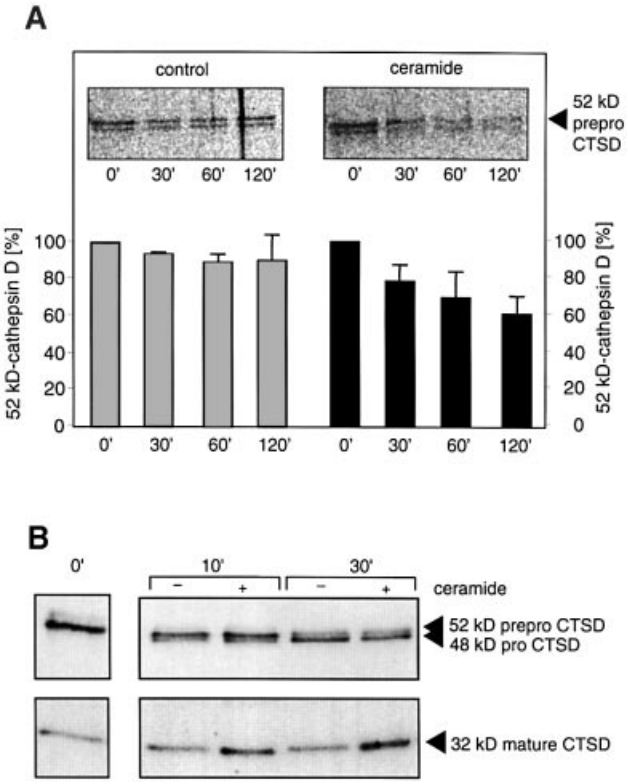

Fig. 8. Ceramide stimulates autoproteolysis of recombinant pre-pro CTSD *in vitro*. (**A**) The cDNA encoding pre-pro CTSD was expressed using the reticulocyte *in vitro* translation systems (Promega) in the presence of [^{35}S]methionine. Aliquots of 0.5 µl radiolabeled recombinant pro CTSD protein were added to 20 µl reaction mixture at pH 4.2 containg 0.75% (w/v) Triton X-100. After incubation with 60 µM D-*erythro*-C_6-ceramide at 37°C for the times indicated, samples were subjected to SDS–PAGE and the radioactive protein detected using the FUJIX-BAS 1000 Bioimager. The insert shows representative results, the quantitative data of three independent experiments are depicted as black and gray columns for ceramide and solvent-treated samples, respectively. (**B**) Ceramide-induced processing of native CTSD was analyzed in lysates from HeLa cells overexpressing recombinant pre-pro CTSD in acidic buffer. Aliquots were left untreated or were incubated in the presence of C_6-ceramide for the times indicated. Expression of CTSD isoforms was detected by Western blotting using polyclonal anti-CTSD antibodies. The lower panel containing the 32 kDa CTSD is a longer exposure of the same blot showing the precursor forms in the upper panel. The result is representative of three independent experiments.

the 52 kDa pre-pro CTSD isoform, indicating a reduction in CTSD processing. In contrast, using the ceramide-synthase-inhibitor fumonisin B1 (Merrill *et al*., 1993) significant changes in CTSD maturation could not be observed (data not shown), suggesting that the A-SMase-generated rather than ceramide-synthase-generated ceramide levels are involved in CTSD maturation.

Discussion

In the present report we have identified the aspartic protease CTSD as a novel intracellular target protein for the lipid second messenger ceramide. We show that ceramide specifically binds to and induces CTSD proteolytic activity. A-SMase-deficient cells derived from Niemann–Pick patients show decreased CTSD activity that was reconstituted by transfection with A-SMase cDNA. Ceramide accumulation in cells derived from A-ceramidase-defective Farber patients correlates with enhanced CTSD activity. These findings suggest that A-SMase-derived ceramide targets endolysosomal CTSD.

The interaction of ceramide with CTSD was revealed by the binding of CTSD to and specific elution from a ceramide-affinity matrix. The ceramide specificity of binding to CTSD was demonstrated by competition analysis employing the UV-crosslinking ceramide analog [^{125}I]TID-ceramide, showing that CTSD specifically binds the naturally occurring D-*erythro*-ceramide but not the functionally inactive analogs D-*erythro*-dihydroceramide, D-*erythro*-dihydrosphingosine or other unrelated lipids, suggesting a specific role for ceramide in CTSD activation. Notably, D-*erythro*-sphingosine, but not the fatty acid palmitate, competed for TID-ceramide binding to CTSD. The length of the alkyl chain in ceramide had no effect. These observations suggest that the alkyl chain rather than the acyl chain in ceramide is important for the interaction with CTSD.

A specific ceramide binding site within CTSD remains to be delineated. Since all three CTSD isoforms, the 52 kDa pre-pro, 48 kDa pro and 32 kDa mature CTSD, eluted from the ceramide-affinity column, the ceramide-binding domain obviously resides within the C-terminal 32 kDa peptide. This assumption is further supported by the [^{125}I]TID-ceramide binding to mature 32 kDa CTSD isolated from human liver.

Based on the ceramide effects on protein kinases Raf-1 and PKCζ (Müller *et al*., 1995, 1998; Huwiler *et al*., 1996), it was speculated that the conserved C1 and C2 domains in the regulatory part of PKC isoenzymes are candidates for lipid interaction motifs. The C1 domains contain tandem repeats of cysteine-rich motifs, a so-called zinc butterfly, which is believed to represent the DAG and phorbol ester binding site (Newton, 1995). The C2 domain in conventional PKC isoenzymes contains a Ca^{2+}-phospholipid-binding domain (CaLB domain), responsible for the interaction with phospholipids. Since DAG did not effectively compete for TID-ceramide binding to CTSD, lipid-binding motifs similar to C1 or C2 domains seem not to be involved in ceramide binding to CTSD. We are currently examining mutations within the CTSD gene to delineate the ceramide-binding domain.

Ceramide is shown to stimulate the enzymatic activity of CTSD in intact cells as assessed by employing a cell-permeable fluorescent dipeptide substrate. The specificity of the fluorescent substrate for CTSD was revealed in fibroblasts from CTSD-deficient mice and $CTSD^{-/-}$ fibroblasts transfected with CTSD cDNA. The possible involvement of other ceramide-responsive enzymes in cellular CTSD activation, however, cannot be ruled out when ceramide effects are studied in intact cells. A cell-free assay was, therefore, established to measure ceramide action on CTSD activity directly. The use of PTH as substrate and a mAb specific for the 1–34 PTH peptide to detect proteolysis of the 1–84 PTH by immunoblotting allowed the quantitative estimation of CTSD enzymatic activity. Fibroblasts from $CTSD^{-/-}$ mice again served as a control for the specificity of the assay. Both endogenous CTSD in cellular lysates and purified mature CTSD responded to D-*erythro*-ceramide but not to D-*erythro*-dihydroceramide with enhanced enzymatic activity. Importantly, D-*erythro*-sphingosine is also able to bind to

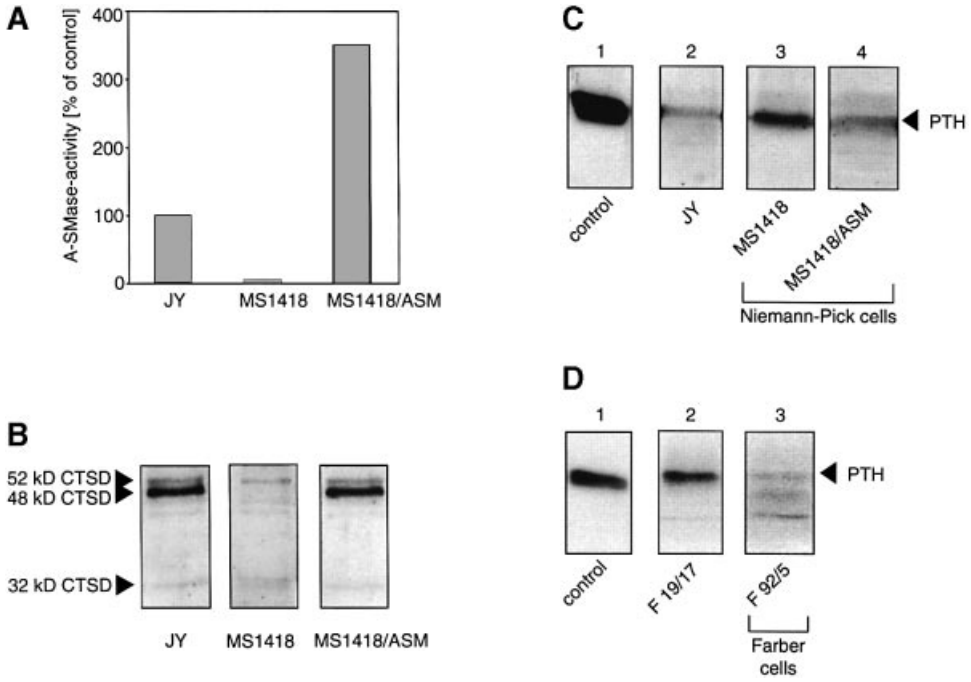

Fig. 9. CTSD maturation and activity in A-SMase- and A-ceramidase-deficient cells. To analyze the effect of A-SMase expression in Niemann–Pick lymphoblasts on CTSD activity, MS1418 NPD cells were transfected with vector control or pRK-ASM. (**A**) JY lymphoblasts and the transfectants were analyzed for A-SMase activity in a micellar *in vitro* assay using [^{14}C]sphingomyelin as substrate. (**B**) CTSD expression in JY, MS 1418 and MS 1418 A-SMase overexpressing cells was analyzed by immunoblotting using polyclonal anti-CTSD antibodies. (**C**) Enzymatic CTSD activity was assayed in lysates of the JY, MS 1418 and MS 1418 A-SMase transfected cells using PTH as substrate by immunoblotting using anti-PTH antibody. (**D**) The effect of A-ceramidase deficiency on CTSD activity was analyzed in fibroblasts derived from Farber disease patients (F92/5, lane 3), in comparison with control fibroblasts (F19/17) expressing normal levels of A-ceramidase (lane 2). PTH was used as substrate for endogenous CTSD activity as in (C).

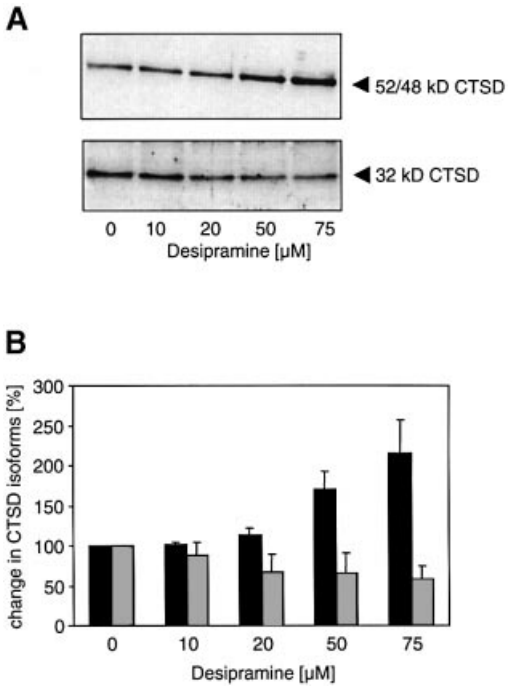

Fig. 10. CTSD maturation is blocked by desipramine. (**A**) HeLa cells overexpressing pre-pro CTSD were left untreated or were pretreated with 10–75 μM desipramine. (**B**) CTSD levels were analyzed by two-dimensional laser scanning (Molecular Dynamics Personal Densitometer) and the changes in 52/48 kDa pro CTSD and mature 32 kDa CTSD isoforms estimated using the PC-BAS TINA program (Raytest) and calculated as a percentage increase over untreated controls. The result of three independent experiments (± SEM) is shown in (B).

and activate CTSD, only when applied in DMSO or Triton X-100 micelles, however. When sphingosine was presented to CTSD as a component of a liposomal lipid bilayer in the absence of detergent, sphingosine lost its ability to activate the enzyme. In contrast, D-*erythro*-ceramide retained its stimulatory effect when incorporated into phosphatidylcholine (PC) liposomes. Since PC liposomes mimic the conditions of lipid bilayers, these observations suggest that ceramide in its membrane-bound form is the physiological activator of CTSD. The acyl chain in ceramide is important for membrane association and the alkyl chain for interaction with the protein. This model implies that ceramide, through protrusion of an alkyl chain, interacts with the hydrophobic cavity of CTSD, as suggested recently (Krönke, 1997). Together, our results identify CTSD as the first protease to be directly and specifically activated by the lipid second messenger ceramide.

In addition, *in vitro* expression of recombinant 52 kDa pre-pro CTSD revealed that ceramide is capable of inducing accelerated autoproteolysis of the pre-pro CTSD isoform. As a possible explanation, ceramide binding to CTSD may lead to a conformational change in the inactive proenzyme, eventually resulting in refolding of the CTSD propeptide that masks the active site of the enzyme (Beyer and Dunn, 1996).

By employing cells that carry genetic defects in the A-SMase gene (Niemann–Pick type A), A-SMase transfection and A-ceramidase-deficient fibroblasts from Farber disease patients, evidence was provided for a functional link between A-SMase, intracellular ceramide and CTSD activity. We demonstrate here that endogenous ceramide

levels in endolysosomal compartments regulate CTSD post-transcriptional maturation as well as enzymatic activity. Thus the aspartic protease CTSD represents the first ceramide-binding protein that colocalizes with A-SMase within the endolysosomal compartment.

The functional significance of ceramide-induced CTSD activation in acidic compartments can be deduced from the main physiological functions of CTSD. The essential function of CTSD for cellular homeostasis and survival is documented in CTSD-deficient mice, which die at around day 26 in a state of anorexia, developing atrophy of the ileal mucosa, progressing towards intestinal necrosis accompanied by thromboembolisms and profound destruction of lymphoid cells (Saftig *et al*., 1995). Bulk lysosomal proteolysis was maintained in these animals; thus the vital physiological function of CTSD resides in the activation or inactivation of hormone-like acid phosphatase, PTH, hemorphin-peptides and angiotensin I (Hamilton *et al*., 1986; Diment *et al*., 1989; Tanaka *et al*., 1990; Katawa *et al*., 1996; Fruitier *et al*., 1998), as well as major histocompatibility complex (MHC) II antigen processing (van der Drift *et al*., 1990; Lutz *et al*., 1997), androgen receptor hydrolysis (Mordente *et al*., 1998) or processing of microtubuli-associated proteins tau and MAP-2 (Johnson *et al*., 1991; Kenessey *et al*., 1997). Limited proteolysis of these substrates in the endosomal and/or lysosomal compartment results in maturation and secretion. It will be interesting to delineate further the biological significance of ceramide-induced activation of CTSD to one or other of these vital biological functions.

A regulatory function of cytokines such as TNF and IFN-γ in the modulation of CTSD isoform expression has been suggested previously (Deiss *et al*., 1996). We observed similar effects of TNF on CTSD maturation in U937, B lymphoblasts and HeLa cells (data not shown). In light of the capability of TNF to stimulate ceramide production in endolysosomal compartments (Schütze *et al*., 1992; Wiegmann *et al*., 1994, 1999; Schwandner *et al*., 1998), it is tempting to speculate that TNF may induce CTSD maturation and activation via A-SMase-generated ceramide. Recent data suggested that TNF-induced A-SMase activation is coupled to the 'death domain' pathway of the p55 TNF receptor (TR55), mediated via the adaptor proteins TRADD and FADD (Wiegmann *et al*., 1994, 1999; Schwandner *et al*., 1998). The results of our study suggest that the endolysosomal protease CTSD is a novel member of the TNF-induced TRADD/FADD/A-SMase pathway. As to the question of how cytokines such as TNF could signal A-SMase-induced CTSD activation, recent evidence indicated that internalization of TR55 is required for A-SMase activation (Schütze *et al*., 1999). TR55-bearing endosomes may fuse with *trans*-Golgi vesicles containing A-SMase, as well as the 52 kDa pre-pro CTSD. A-SMase-derived ceramide may then bind to and activate the inactive pre-pro CTSD to generate the 48/32 kDa active mature CTSD isoforms.

The role of A-SMase and ceramide in apoptosis is rather controversial. The results of this study suggest that CTSD may couple A-SMase-derived ceramide to the apoptotic pathway. An apoptotic potential of CTSD has recently been inferred from employing antisense CTSD mRNA, which protected HeLa cells from IFN-γ-, TNF- and Fas/APO-1-induced apoptosis (Deiss *et al*., 1996). In addition, fibroblasts derived from CTSD-deficient mice showed a reduced apoptotic response to etoposide and adriamycin treatment (Wu *et al*., 1998). CTSD is also involved in the apoptotic cascade in PC12 cells following serum deprivation (Shibata *et al*., 1998; Ohsawa *et al*., 1999). Our own unpublished observations suggest that CTSD is able to cleave pro-caspase 3. This finding may explain the previous notions that ceramide is upstream of CPP32 (caspase 3; Mizushima *et al*., 1996; Smyth *et al*., 1996; Anjum *et al*., 1998; Yoshimura *et al*., 1998), where CTSD would be the missing link between ceramide and caspase 3. Indeed, translocation of CTSD from endolysosomal compartments has been demonstrated after treating cells with oxidized LDL (Yuan *et al*., 1997; Li *et al*., 1998) or in response to oxidative stress (Brunk *et al*., 1997; Roberg and Öllinger, 1998). Thus, ceramide-activated CTSD may have access to cytosolic substrates such as caspases including CPP32.

Materials and methods

Cells, mice and reagents

U937, HeLa and HEK 293 cells were obtained from ATTC and maintained in CLICK's RPMI culture medium (Biochrome) supplemented with 10% fetal calf serum (FCS), 10 mM glutamine, 0.1 mM β-mercaptoethanol and 50 μg/ml each of streptomycin and penicillin. EBV-transfected human lymphoblasts JY and EBV-transfected human lymphoblasts from Niemann–Pick patients (clones MS1418 and MS1271) were kindly provided by D.Green (La Jolla, CA). Fibroblasts from Farber disease patients were kindly provided by K.Sandhoff and G.van Echten (Bonn, Germany). CTSD-deficient mice (C57BL/6 $CTSD^{-/-}$) and $CTSD^{-/-}$ fibroblasts were kindly provided by Dr Saftig, Göttingen (Saftig *et al*., 1995). Progeny of heterozygous CTSD-deficient mice were genotyped by PCR of genomic DNA from tail biopsies as described previously (Saftig *et al*., 1996).

In vitro expression of pre-pro CTSD

The cDNA encoding human pre-pro CTSD (Faust *et al*., 1985) was obtained by PCR using a cDNA library from U937 cells and subcloned into pRK5 (provided by D.Goeddel, Tularik Inc., San Francisco, CA). Oligonucleotides used for PCR were (5′-CCGCCATGCAGCCCTCC-AGC-3′) and (5′-GACTCTCCTCTGTTTCTGTGC-3′).

In vitro expression of the CTSD cDNA was performed in the reticulocyte *in vitro* translation systems (Promega) in the presence of [^{35}S]methionine for 1 h at 32°C following the manufacturer's protocol.

Retroviral transfections with A-SMase and CTSD cDNA

The cDNAs of human A-SMase and human pre-pro CTSD were subcloned into the retroviral vector pLSXN or pBabe puro, respectively. Transient transfection of the retroviral producer line FLYA13 (Cosset *et al*., 1995) was performed by calcium phosphate precipitation with 10 μg pLXSN-ASMase or pLXSN-CTSD and 5 μg pCMV/VSV-G expressing the G protein of vesicular stomatitis virus to produce pseudotyped amphotropic retroviral particles. Cells (1×10^6) were plated on 100-mm dishes in DMEM without HEPES the night before transfection. The medium was changed 12 h post-transfection. Transduction of MS1418 Niemann–Pick lymphoblasts or $CTSD^{-/-}$ fibroblasts was performed by incubating 5×10^4 cells with recombinant viral supernatant harvested 48 h post-transfection and containing 8 μg/ml polybrene at 37°C overnight. Transduced cells were selected by G418 for 10–14 days (MS1218 lymphoblasts) or with puromycin for 4–6 days ($CTSD^{-/-}$ fibroblasts) and pooled cell populations were used for further experiments.

Ceramide-affinity chromatography and immunoblotting

Generation of the affinity matrix. Activated CH–Sepharose 4B (4 g; Amersham Pharmacia Biotech) was resuspended in 1 mM HCl and subsequently transferred to 30, 70 and 100% tetrahydrofuran (THF). D-*erythro*-sphingosine (50 mg; Sigma) in 6 ml anhydrous THF was coupled to activated CH–Sepharose 4B following the addition of 100 μl *N*-ethylmorpholine. The reaction between the *N*-hydroxysuccinimide ester in the activated CH–Sepharose 4B and the amine in sphingosine resulted in the formation of an amide bond and release of

N-hydroxysuccinimide. After 15 h incubation at 4°C, the beads were washed in 100% THF and residual active sites were blocked by ethanolamine (2 h at room temperature). After washing three times in 100% THF followed by three times in H_2O, the ceramide-affinity matrix (~10 ml packed volume) was filled in column XK 16/20 (Pharmacia Biotech).

The efficiency of sphingosine coupling was estimated by using a related radiolabeled compound, *N*-([^{14}C]6-aminohexanoyl)-D-*erythro*-sphingosine (4.0 mg; 0.288×10^6 d.p.m.). Incubation was performed with ~600 µl (corresponding to ~200 mg freeze-dried material) of activated CH–Sepharose 4B in anhydrous THF in the presence of 10 µl triethylamine. After incubation at 4°C for 3 h, 50 µl of ethanolamine were added and incubation was continued for 2 h. The gel was then transferred onto a filter and washed with THF, methanol and 1 mM HCl. Scintillation counting revealed that under the above coupling conditions at least 86% of the amino-group-containing ligand became covalently bound to the Sepharose matrix.

Affinity chromatography of cellular lysates. U937 cells (2×10^8) were homogenized in 1 ml buffer H [150 mM KCl, 5 mM NaF, 1 mM phenylmethylsulfonylfluoride, 20 µM pepstatin, 20 µM leupeptin, 20 µM antipain (Boehringer Complete, 1:100) in 40 mM HEPES pH 7.4] by passing the cells through a 28 G needle followed by 3× sonication for 10 s. Lysates were cleared by centrifugation (5 min, 1000 *g*), the supernatant adjusted to 0.075% (v/v) Triton X-100 and membrane proteins solubilized for 30 min. After centrifugation for 1 h at 100 000 *g*, the supernatants, containing 25–30 mg protein, were loaded onto the ceramide-affinity column by recirculating for 15 h at 4°C at a flow rate of 10 ml/h. The column was washed in buffer H containing 0.075% Triton X-100, and the bound proteins eluted with 100 µM D-*erythro*-ceramide in buffer H containing 0.075% Triton X-100. Eluted proteins were concentrated, separated by 10% SDS–PAGE and further analyzed by immunoblotting using the Mini-Transblot (Biometra, Göttingen, Sweden) and the 'enhanced chemiluminescence' (ECL) system (Amersham Pharmacia Biotech).

[^{125}I]TID-ceramide UV-crosslinking and competition analysis

Radiolabeling of TID-ceramide. *N*-[3-[[[2-(tributylstannyl)-4-[3-(trifluoromethyl)-3H-diazerin-3-yl]benzyl]oxy]carbonyl]propanoyl]D-*erythro*-sphingosine (tin precursor of TID-ceramide) was synthesized and purified by HPLC as described previously (Weber and Brunner, 1995). Radiolabeling was performed by incubating 200 nmol tin-ceramide in 20 µl acetic acid, 5 mCi of Na^{125}I and 5 µl of peracetic acid (32% in acetic acid) as described previously (Weber and Brunner, 1995). Radiolabeled lipid was extracted with chloroform–methanol and subjected to thin-layer chromatography (TLC) using as solvent chloroform/methanol (95:5). [^{125}I]TID-ceramide was identified by autoradiography, extracted with THF, dissolved in toluene–ethanol and stored at –20°C.

Photoaffinity labeling. Purified CTSD from human liver (2 µg; Sigma) was incubated with 1 µCi (0.5 pmol) of [^{125}I]TID-ceramide in 20 µl buffer H containing 0.075% Triton X-100 for 5 min at 37°C in the absence or presence of competitor lipids. Photo-crosslinking was performed by UV irradiation (2 min, 100 W at 365 nm) using a UVP Model B100A Black Ray Lamp (Herolab, Wiesloch, Germany). Radiolabeled protein was analyzed after separation on 12.5% SDS–PAGE by autoradiography using the Fuji BAS 1000 Bioimager (Raytest) and quantitated using the PC-BAS TINA program (Raytest).

CTSD assays

Cellular CTSD activity was assayed by using the CellProbe GL*cathepsin D enzyme substrate (Coulter) and proteolysis of the peptide glycine–leucine–Rho 110 resulting in the formation of fluorescence which was estimated by flow cytometry (Becton-Dickinson FACSCalibur). Briefly, cells were washed with phosphate-buffered saline (PBS) and resuspended at a concentration of 3×10^6 cells/ml in PBS. Aliquots of 50 µl were incubated for 5 min at 37°C, 25 µl of the CellProbe reagent were added and incubation continued for 1 min at 37°C. The reaction was stopped on ice and 1 ml cold PBS was added prior to FACS analysis.

CTSD autoproteolysis assays. For analysis of autoproteolysis of recombinant pre-pro CTSD, 0.5 µl aliquots of radiolabeled recombinant proteins were added to 20 µl reaction mixture at pH 4.2 containing 0.75% (w/v) Triton X-100. After incubation in the absence or presence of 60 µM C_6-ceramide at 37°C for indicated times, samples were subjected to SDS–PAGE and the radioactive proteins were analyzed using the FUJIX-BAS 1000 Bioimager and PC-BAS TINA software for quantitation.

Autoproteolysis of native, endogenous pre-pro CTSD was analyzed by incubating 2 µg of U937 lysates, or lysates from transiently transfected CTSD-overexpressing HeLa cells, for the indicated times at 37°C in 20 µl acidic buffer (100 mM sodium acetate, 100 mM potassium chloride pH 4.2). Assays were performed with or without D-*erythro*-C_6-ceramide or D-*erythro*-C_6-dihydroceramide dissolved in DMSO or integrated in phosphatidylcholine liposomes at 10 mol% (1 mM). Reactions were stopped by boiling the samples with Tris–tricine–SDS–sample buffer (2% β-mercaptoethanol, 12% glycerol, 50 mM Tris pH 6.8, 4% sodium dodecyl sulfate, 0.01% Coomassie G).

Protein was separated on 12.5% SDS–PAGE and transferred onto nitrocellulose filters. Immunoblotting was performed with polyclonal anti-CTSD antibody (Calbiochem), filters were washed with TBST and incubated with a 1:10 000 dilution of anti-rabbit horseradish peroxidase conjugate (Kodak) in TBST buffer. Filters were washed and developed using the ECL detection reagent (Amersham).

Functional CTSD assay. To estimate the activity of purified human liver CTSD (Sigma) or cellular CTSD, 2 µg lysate–protein or 50 ng human liver CTSD were incubated for the indicated times with 50 ng PTH at 37°C in a volume of 20 µl acidic buffer (100 mM sodium acetate, 100 mM potassium chloride pH 4.2). Stimulation was performed with D-*erythro*-C_6-ceramide, D-*erythro*-C_6-dihydroceramide, D-*erythro*-sphingosine, D-*erythro*-dihydrosphingosine or palmitate, either dissolved in DMSO or integrated into PC liposomes to mimic the *in vivo* detergent-free conditions at a ratio of 10 mol% (final concentration 9 mM phosphatidylcholine/1 mM ceramide). The concentration of lipids in the low millimolar range was reported as being optimal for measuring CTSD activity (Watanabe and Yago, 1983) and glucosidase activity (Wilkening *et al*., 1998).

Proteins were separated by SDS–PAGE and immunoblotting performed using anti-PTH mAb specific for fragment 1–34 (Biogenesis) and a secondary horseradish peroxidase conjugate. Blots were developed using the ECL detection reagent (Amersham).

A-SMase assay

A-SMase activity was assayed in a micellar *in vitro* assay using ^{14}C-labeled sphingomyelin (Amersham) as substrate as described previously (Wiegmann *et al*., 1994). Briefly, 3×10^6 cells were homogenized, in triplicate, in 0.2% Triton X-100, and 50 µg of protein from the cellular lysates were assayed for A-SMase activity in a buffer (50 µl final volume) containing 250 mM sodium acetate, 1 mM EDTA (pH 5.0) and 2.25 µl [*N*-methyl-^{14}C]sphingomyelin. Phosphorylcholine was then extracted with 800 ml chloroform–methanol (2:1 v/v) and 250 µl of H_2O, and the amount of radioactive phosphorylcholine produced from hydrolysis of [^{14}C]sphingomyelin determined in the aqueous phase by scintillation counting.

Acknowledgements

This study was performed in partial fulfillment of the PhD thesis of M.Wickel. We thank Andrea Hethke and Gudrun Scherer for exellent technical assistance, K.Bernardo for helpful discussions, R.Pohlmann for the generous gift of anti-murine CTSD antibodies, P.Saftig and C.Peters for supplying the CTSD-deficient mice, K.Sandhoff and G.van Echten for supplying A-SMase c-DNA and fibroblasts from Farber patients, and D.Green for supplying NPA lymphoblasts. This work was supported by grants from the Deutsche Forschungsgemeinschaft (SFB 415), the Bundesministerium für Bildung und Forschung and the Swiss National Science Foundation.

References

Adam-Klages,S., Adam,D., Wiegmann,K., Struve,S., Kolanus,W., Schneider-Mergener,J. and Krönke,M. (1996) FAN, a novel WD-repeat protein, couples the p55 TNF-receptor to neutral sphingomyelinase. *Cell*, **86**, 937–947.

Anjum,R., Ali,A.M., Begum,Z., Vanaja,J. and Khar,A. (1998) Selective involvement of caspase 3 in ceramide induced apoptosis in AK-5 tumor cells. *FEBS Lett.*, **439**, 81–84.

Beyer,B.M. and Dunn,B.M. (1996) Self-activation of recombinant human lysosomal procathepsin D at a newly engineered cleavage junction, 'short' pseudocathepsin D. *J. Biol. Chem.*, **271**, 15590–15596.

Bielawska,A., Crane,H.M., Liotta,D., Obeid,L. and Hannun,J. (1993) Selectivity of ceramide-mediated biology. Lack of activity of *erythro*-dihydroceramide. *J. Biol. Chem.*, **268**, 26226–26232.

Brunk,U.T., Dalen,H., Roberg,K. and Hellquist,H.B. (1997) Photo-oxidative disruption of lysosomal membranes causes apoptosis of cultured human fibroblasts. *Free Radical Biol. Med.*, **23**, 616–626.

Cifone,M.G., De Maria,R., Roncaioli,P., Rippo,M.R., Azuma,M., Lanier,L.L., Santoni,A. and Testi,R. (1995) Apoptotic signaling through CD95 (Fas/APO-1) activates an acidic sphingomyelinase. *J. Exp. Med.*, **177**, 1547–1552.

Conner,G.E. (1989) Isolation of procathepsin D from mature cathepsin D by pepstatin affinity chromatography. Autocatalytic proteolysis of the zymogen form of the enzyme. *Biochem. J.*, **263**, 601–604.

Cosset,F.-L., Takeuchi,Y., Battini,J.-L., Weiss,R.A. and Collins,M.K.L. (1995) High-titer packaging cells producing recombinant retroviruses resistant to human serum. *J. Virol.*, **69**, 7430–7436.

Deiss,L.P., Galinka,H., Berissi,H., Cohen,O. and Kimchi,A. (1996) Cathepsin D protease mediates programmed cell death induced by interferon-γ, Fas/APO-1 and TNF-α. *EMBO J.*, **15**, 3861–3870.

De Maria,R., Rippo,M.R., Schuchmann,E.H. and Testi,R. (1998) Acidic sphingomyelinase (ASM) is necessary for FAS-induced GD3 ganglioside accumulation and efficient apoptosis in lymphoid cells. *J. Exp. Med.*, **187**, 897–902.

Diment,S., Martin,K.L. and Stahl,P.D. (1989) Cleavage of parathyroid hormone in macrophage endosomes illustrates a novel pathway for intracellular processing of proteins. *J. Biol. Chem.*, **264**, 13403–13406.

Dobrowski,R.T., Kamibayashi,C., Mumby,M.C. and Hannun,Y. (1993) Ceramide activates heterotrimeric protein phosphatase 2A. *J. Biol. Chem.*, **268**, 15523–15530.

Faust,P.L., Kornfeld,S. and Chirgwin,J.M. (1985) Cloning and sequence analysis of cDNA for human cathepsin D. *Proc. Natl Acad. Sci. USA*, **82**, 4910–4914.

Fruitier,I., Garreau,I. and Piot,J.M. (1998) Cathepsin D is a good candidate for the specific release of stable hemorphin from hemoglobin *in vivo*: VV-hemorphin-7. *Biochem. Biophys. Res. Commun.*, **246**, 719–724.

Gieselmann,V., Pohlmann,R., Hasilik,A. and von Figura,K. (1983) Biosynthesis and transport of cathepsin D in cultured human fibroblasts. *J. Cell Biol.*, **97**, 1–5.

Haimovitz-Friedmann,A. *et al.* (1997) Lipopolysaccharide induces disseminated endothelial apoptosis requiring ceramide generation. *J. Exp. Med.*, **186**, 1831–1841.

Hamilton,J.W., MacGregor,R.R. and Jilka,R.L. (1986) Formation of parathormone 8–34 by cathepsin D digestion of parathormone and its efficacy as a hormone antagonist. *Mol. Cell. Endocrinol.*, **44**, 179–183.

Hannun,Y.A. and Obeid,L.M. (1995) Ceramide: an intracellular signal for apoptosis. *Trends Biochem. Sci.*, **20**, 73–77.

Herr,I., Wilhelm,D., Böhler,T., Angel,P. and Debatin,K.-M. (1997) Activation of CD95 (APO-1/Fas) signaling by ceramide mediates cancer therapy-induced apoptosis. *EMBO J.*, **16**, 6200–6208.

Huang,C., Ma,W., Ding,M., Bowden,G.T. and Dong,Z. (1997) Direct evidence for an important role of sphingomyelinase in ultraviolet-induced activation of c-*jun* N-terminal kinase. *J. Biol. Chem.*, **272**, 27753–27757.

Hurwitz,R., Ferlinz,K. and Sandhoff,K. (1994) The tricyclic anti-depressant desipramine causes proteolytic degradation of lysosomal sphingomyelinase in human fibroblasts. *Biol. Chem. Hoppe Seyler*, **375**, 447–450.

Huwiler,A., Brunner,J., Hummel,R., Vervoodeldonk,M., Stabel,S., van den Bosch,H. and Pfeilschifter,J. (1996) Ceramide binding and activation defines protein kinase c-Raf as a ceramide-activated protein kinase. *Proc. Natl Acad. Sci. USA*, **93**, 6959–6963.

Johnson,G.V., Litersky,J.M. and Whitaker,J.N. (1991) Proteolysis of microtubule-associated protein 2 and tubulin by cathepsin D. *J. Neurochem.*, **57**, 1577–1583.

Katawa,L.C., Tyagi,S.C., Cambell,S.E., Lee,S.J., Cicila,G.T. and Weber,K.T. (1996) Valvular interstitial cells express angiotensinogen and cathepsin D and generate angiotensin peptides. *Int. J. Biochem. Cell Biol.*, **28**, 807–821.

Kenessey,A., Nacharaju,P., Ko,L.W. and Yen,S.H. (1997) Degradation of tau by lysosomal enzyme cathepsin C: implication for Alzheimer neurofibrillary degeneration. *J. Neurochem.*, **69**, 2026–2038.

Kolesnick,R.N. and Krönke,M. (1998) Regulation of ceramide production and apoptosis. *Annu. Rev. Physiol.*, **60**, 643–665.

Kreder,D. *et al.* (1999) Impaired neutral sphingomyelinase activation and cutaneous barrier repair in FAN-deficient mice. *EMBO J.*, **18**, 2472–2479.

Krönke,M. (1997) The mode of ceramide action: the alkyl chain protrusion model. *Cytokine Growth Factor Rev.*, **8**, 103–107.

Law,B. and Rossie,S. (1995) The dimeric and catalytic subunit forms of PP2A from rat brain are stimulated by C_2 ceramide. *J. Biol. Chem.*, **270**, 12808–12813.

Li,W., Yuan, X.M., Olsson,A.G. and Brunk,U.T. (1998) Uptake of oxidized LDL by macrophages results in partial lysosomal enzyme inactivation and translocation. *Arterioscler. Thromb. Vasc. Biol.*, **18**, 177–184.

Liu,B., Obeid,L.M. and Hannun,Y.A. (1997) Sphingomyelinases in cell regulation. *Semin. Cell Dev. Biol.*, **8**, 311–322.

Liu,P. and Anderson,G.G.W. (1995) Compartmentalized production of ceramide at the cell surface. *J. Biol. Chem.*, **270**, 27179–27185.

Lutz,M.B. *et al.* (1997) Intracellular routes and selective retention of antigens in mildly acidic cathepsin D/lysosome-associated membrane protein-1/MHC Class II-positive vesicles in immature dendritic cells. *J. Immunol.*, **159**, 3707–3716.

Mathias,S., Dressler,K.A. and Kolesnick,R.N. (1991) Characterization of a ceramide-activated protein kinase: stimulation by tumor necrosis factor α. *Proc. Natl Acad. Sci USA*, **88**, 1009–10013.

Merrill,A.H.,Jr, Wang,E., Gilchrist,D.G. and Riley,R.T. (1993) Fumonisins and other inhibitors of *de novo* sphingolipid biosynthesis. *Adv. Lipid Res.*, **26**, 215–234.

Metcalf,P. and Fusek,M. (1993) Two crystal structures for cathepsin D: the lysosomal targeting signal and active site. *EMBO J.*, **14**, 1293–1302.

Mizushima,N., Koike,R., Kohsaka,H., Kushi,Y., Handa,S., Yagita,H. and Miyasaka,N. (1996) Ceramide induces apotosis via CPP32 activation. *FEBS Lett*, **395**, 267–271.

Monney,L., Olivier,R., Otter,I., Jansen,B., Poirier,G.G. and Borner,C. (1998) Role of an acidic compartment in tumor necrosis factor α-induced production of ceramide, activation of caspase-3 and apoptosis. *Eur. J. Biochem.*, **251**, 295–303.

Mordente,J.H., Choudhury,M.S., Tazaki,H., Mallouh,C. and Konno,S. (1998) Hydrolysis of androgen receptor by cathepsin D: its biological significance in human prostate cancer. *Br. J. Urol.*, **82**, 431–435.

Müller,G., Ayoub,M., Storz,P., Rennecke,J., Fabbro,D. and Pfizenmaier,K. (1995) PKCζ is a molecular switch in signal transduction of TNFα, bifunctionally regulated by ceramide and arachidonic acid. *EMBO J.*, **14,** 1961–1996.

Müller,G., Storz,P., Bourteele,S., Döppler,H. and Pfizenmaier,K. (1998). Regulation of Raf-1 kinase by TNF via its second messenger ceramide and cross-talk with mitogenic signalling. *EMBO J.*, **17**, 732–742.

Newton,A.C. (1995) Protein kinase C: structure, function and regulation. *J. Biol. Chem.*, **270**, 28495–28498.

Obeid,L.M., Linardic,C.M., Karolak,L.A. and Hannun,J.A. (1993) Programmed cell death induced by ceramide. *Science*, **259**, 1769–1771.

Ohsawa,Y., Isahara,K., Kanamori,S., Shibata,M., Kametaka,S., Gotow,T., Watanabe,T., Kominami,E. and Uchiyama,Y. (1999) An ultrastructural and immunohistochemical study of PC12 cells during apoptosis induced by serum depriviation with special reference to autophagy and lysosomal cathepsins. *Arch. Histol. Cytol.*, **61**, 395–403.

Perry,D.K. and Hannun,Y.A. (1998) The role of ceramide in cell signaling. *Biochim. Biophys. Acta*, **1436**, 233–243.

Rijnboutt,S., Stoorvogel,W., Geuze,H. and Strous,G.J. (1992) Identification of subcellular compartments involved in biosynthetic processing of cathepsin D. *J. Biol. Chem.*, **267**, 15665–15672.

Roberg,K. and Öllinger,K. (1998) Oxidative stress causes relocation of the lysosomal enzyme cathepsin D with ensuing apoptosis in neonatal rat cardiomyocytes. *Am. J. Pathol.*, **152**, 1151–1156.

Saftig,P. *et al.* (1995) Mice deficient for the lysosomal proteinase cathepsin D exhibit progressive atropy of the intestinal mucosa and profound destruction of lymphoid cells. *EMBO J.*, **14**, 3599–3608.

Saftig,P., Peters,C., von Figura,K., Craessaerts,K., Van Leuven,F. and De Strooper,B. (1996) Amyloidogenic processing of human amyloid precursor protein in hippocampal neurons devoid of cathepsin D. *J. Biol. Chem.*, **271**, 27241–27244.

Santana,P. *et al.* (1996) Acid sphingomyelinase-deficient human lymphoblasts and mice are defective in radiation-induced apoptosis. *Cell*, **86**, 189–199.

Schütze,S., Potthoff,K., Machleidt,T., Berkovic,D., Wiegmann,K. and Krönke,M. (1992) TNF activates NF-κB by phosphatidylcholine-specific phospholipase C-induced 'acidic' sphingomyelin breakdown. *Cell*, **71**, 765–776.

Schütze,S., Machleidt,T., Adam,D., Schwandner,R., Wiegmann,K., Kruse,M.-L., Heinrich,M., Wickel,M. and Krönke,M. (1999) Inhibition of receptor internalization by monodansylcadaverine selectively blocks p55 tumor necrosis factor receptor death domain signaling. *J. Biol. Chem.*, **274**, 10203–10212.

Schwandner,R., Wiegmann,K., Bernado,K., Kreder,D. and Krönke,M. (1998) TNF receptor death domain-associated proteins TRADD and FADD signal activation of acid sphingomyelinase. *J. Biol. Chem.*, **273**, 5916–5922.

Shibata,M. *et al.* (1998) Participation of cathepsin D and B in apoptosis of PC12 cells following serum depriviation. *Biochem. Biophys. Res. Commun.*, **251**, 199–203.

Smyth,M.J., Perry,D.K., Zhang,J., Poirier,G.G., Hannun,Y. and Obeid,L.M. (1996) prICE: a downstream target for ceramide-induced apoptosis and the inhibitory action of Bcl-2. *Biochem. J.*, **316**, 25–28.

Spiegel,S. and Merrill,A.H.,Jr (1996) Sphingolipid metabolism and growth regulation. *FASEB J.*, **10**, 1388–1397.

Tanaka,Y., Himeno,M. and Kato,K. (1990) Release of acid phosphatase from lysosomal membranes by cathepsin D. *J. Biochem. (Tokyo)*, **108**, 287–291.

van der Drift,A.C.M., van Noort,J.M. and Krüse,J. (1990) Catheptic processing of protein antigens: enzymatic and molecular aspects. *Semin. Immunol.*, **2**, 255–271.

van Echten-Deckert,G., Klein,A., Linke,T., Heinemann,T., Weisgerber,J. and Sandhoff,K. (1997) Turnover of endogenous ceramide in cultured normal and Farber fibroblasts. *J. Lipid Res.*, **38**, 2569–2579.

Watabe,S. and Yago,N. (1983) Phospholipids activate cathepsin D. *Biochem. Biophys. Res. Commun.*, **110**, 934–939.

Weber,T. and Brunner,J. (1995) 2-(Tributylstannyl)-4-[3-(trifluoromethyl)-3H-diazirin-3-yl]benzyl alcohol: a building block for photolabeling and cross-linking reagents of very high specific radioactivity. *J. Am. Chem. Soc.*, **117**, 3084–3095.

Westwick,J.K., Bielawska,A.E., Dbaibo,G., Hannun,Y.A. and Brenner, D.A. (1995) Ceramide activates the stress-activated protein kinases. *J. Biol. Chem.*, **270**, 22689–22692.

Wiegmann,K., Schütze,S., Machleidt,T., Witte,D. and Krönke,M. (1994) Functional dichotomy of neutral and acidic sphingomyelinase in tumor necrosis factor signaling. *Cell*, **78**, 1005–1015.

Wiegmann,K., Schwandner,R., Krut,O., Yeh,W.-C., Mak,T.W. and Krönke,M. (1999) Requirement of FADD for tumor necrosis factor-induced activation of acid sphingomyelinase. *J. Biol. Chem.*, **274**, 5267–2570.

Wilkening,G., Linke,T. and Sandhoff,K. (1998) Lysosomal degradation on vesicular membrane surfaces. Enhanced glucosylceramide degeneration by lysosomal anionic lipids and activators. *J. Biol. Chem.*, **273**, 30271–03278.

Wu,S.H., Saftig,P., Peters,C. and El-Deiry,W. (1998) Potential role for cathepsin D in p53-dependent tumor suppression and chemosensitivity. *Oncogene*, **16**, 2177–2183.

Yoshimura,S. *et al.* (1998) Ceramide formation leads to caspase-3 activation during hypoxic PC12 cell death. *J. Biol. Chem.*, **273**, 6921–6927.

Yuan,X.M., Li,W., Olsson,A.G. and Brunk,U.T. (1997) The toxicity of oxidized low-density lipoprotein is mediated through lysosomal damage. *Arteriosclerosis*, **133**, 153–161.

Zhang,J., Alter,N., Reed,J.C., Borner,C., Obeid,L.M. and Hannun,Y. (1996) Bcl-2 interrupts the ceramide-mediated pathway of cell death. *Proc. Natl Acad. Sci. USA*, **93**, 5325–5328.

Zhang,Y. *et al.* (1997). Kinase supressor of Ras is ceramide activated protein kinase. *Cell*, **89**, 63–72.

Zull,J.E. and Chuang,J. (1985) Characterization of parathyroid hormone fragments produced by cathepsin D. *J. Biol. Chem.*, **260**, 1608–1613.

Received April 12, 1999; revised and accepted August 3, 1999